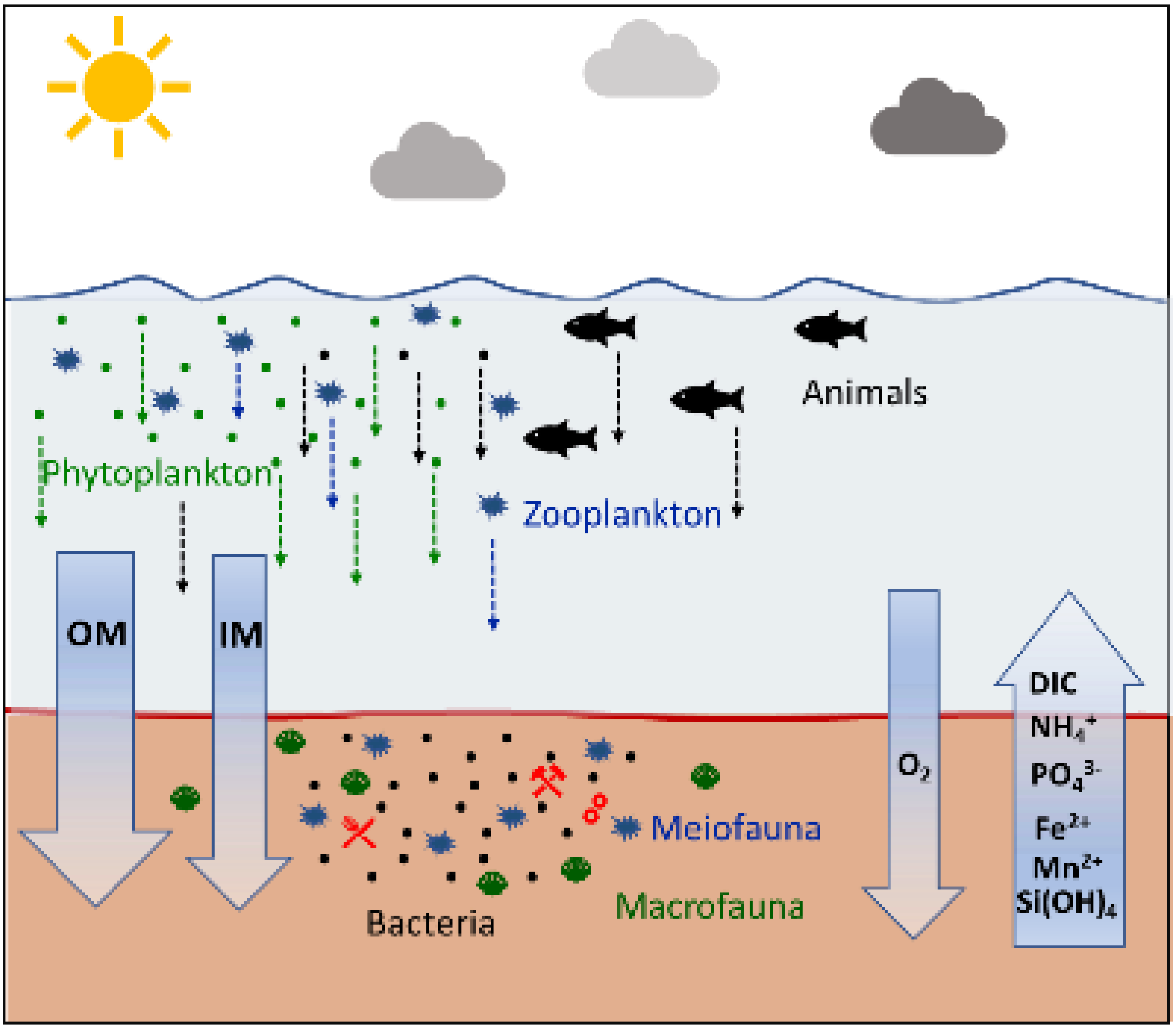

Figure S1. Schematic view of early diagenesis processes.

Bacteria; : macrofauna; : meiofauna; : biogeochemical processes.

OM, Organic Matter; IM, Inorganic Matter; DIC, Dissolved Inorganic Carbon.

a)

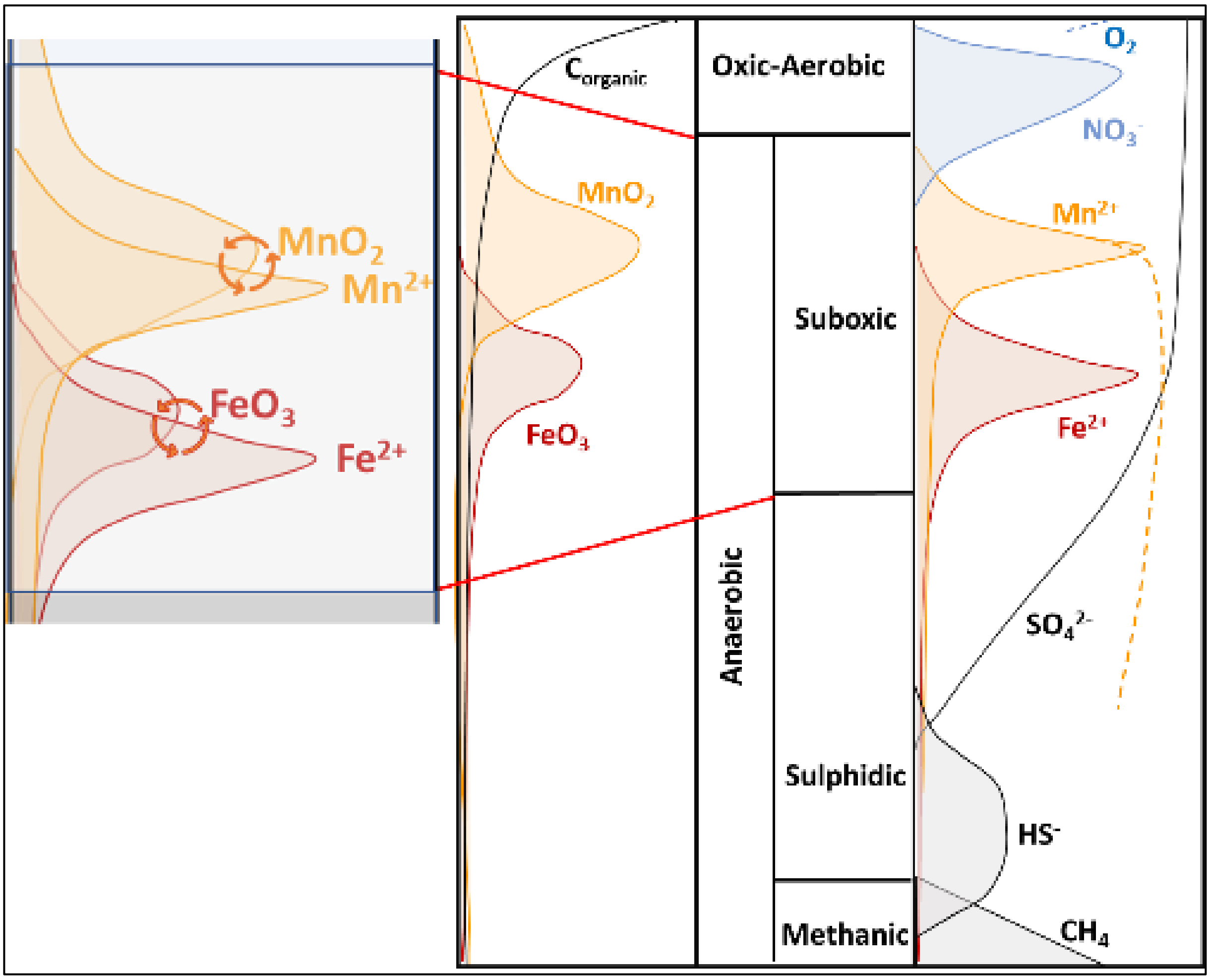

b)

Aerobic biodegradation

- $(CH_2O)106(NH_3)16(H_3PO_4)+138O_2 <=> 106CO_2+16HNO_3+H3PO_4+122H_2O$ — $\Delta G^{o\prime}$ = -3190 kJ/mole of Glucose

Anaerobic biodegradation

Denitrification (Nitrate reduction)

- 3a. (CH20)106 (NH3)16 (H3P04) + 94.4HN03 -> 106CO2 + 55.2N2 + H3P04+ 177.2H20 — $\Delta G^{o\prime}$ = -3030 kJ/mole
- 3b. (CH20)106 (NH3)16 (H3P04) + 84.8HNO3 -> 106CO2 + 42.4N2 + 16NH3+ H3P04 + 148.4H20 — $\Delta G^{o\prime}$ = -2750 kJ/mole

Oxi-hydroxi-Mn-reduction

- $(CH_2O)106(NH_3)16(H_3PO_4)+236MnO_2+472H+<=>236Mn^{2+}106CO_2+8N_2+H_3PO_4^{1}+336H_2O$ — $\Delta G^{o\prime}$=-3090 kJ/mole (Birnessite), -3050 kJ/mole (Nsutite), -2920 kJ/mole (Pyrolusite)

Oxi-hydroxi-Fe reduction

- $(CH_2O)106(NH_3)16(H_3PO_4)+212Fe_2O_3+848H+<=>424Fe^{2+}106CO_2+8NH_3^{-}+H_3PO_4^{3-}+530H_2O$ — $\Delta G^{o\prime}$ = -1110 kJ/mole (HEMATITE, Fe2O3, -1330 kJ/mole (Limonitic GOETHITE, FeOOH)

Sulfate reduction

- $(CH_2O)106(NH_3)16(H_3PO_4)+55SO_4^{2-}<=>106CO_2+16NH_3^{-}+55S^{2-}+H_3PO_4^{3-}+106H_2O$ — $\Delta G^{o\prime}$ = -380 kJ/mole

Methanogenesis

- $(CH_2O)106(NH_3)16(H_3PO_4) <=> 53CH_4+53CO_2+16NH_3+H_3PO_4$ — $\Delta G^{o\prime}$ = -350 kJ/mole

  $CH_{4(aq)}+SO_4^{2-} HS^{-}+HCO_3^{-}+H_2O$ — DG= –34 kJ mol^{-1} CH_4

Figure S2. Early diagenesis processes. a) Schematic drawing of dissolved ions produced and/or consumed in pore waters by early diagenesis processes (modified from Froelich *et al.*, 1979; Milucka *et al.*, 2012). Enlargement: Fe and Mn oxyhydroxide cycles; b) biogeochemical reactions taking place in the top few centimeters of sediment (Blue: final electron acceptors; Red: organic matter degradation products).

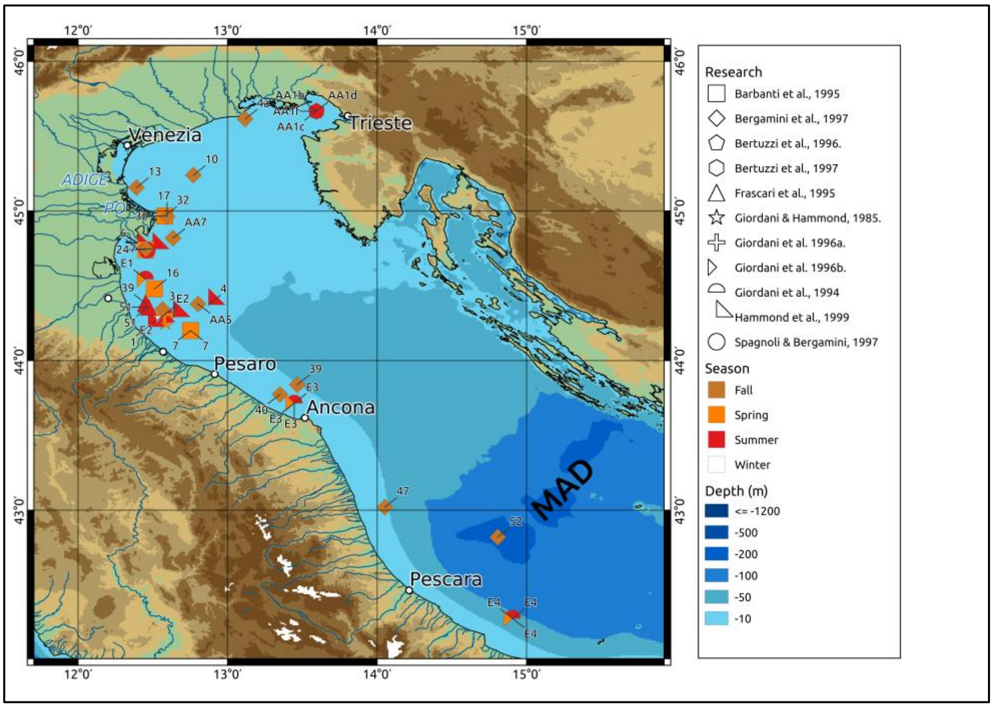

Figure S3. Stations in the Central and Northern Adriatic Sea where *in situ* measurements, on-board core incubations, and pore water chemical profile modeling were conducted from 1982. Symbols, season, and depth color codes are reported in the legend, stations are listed in Table S1.

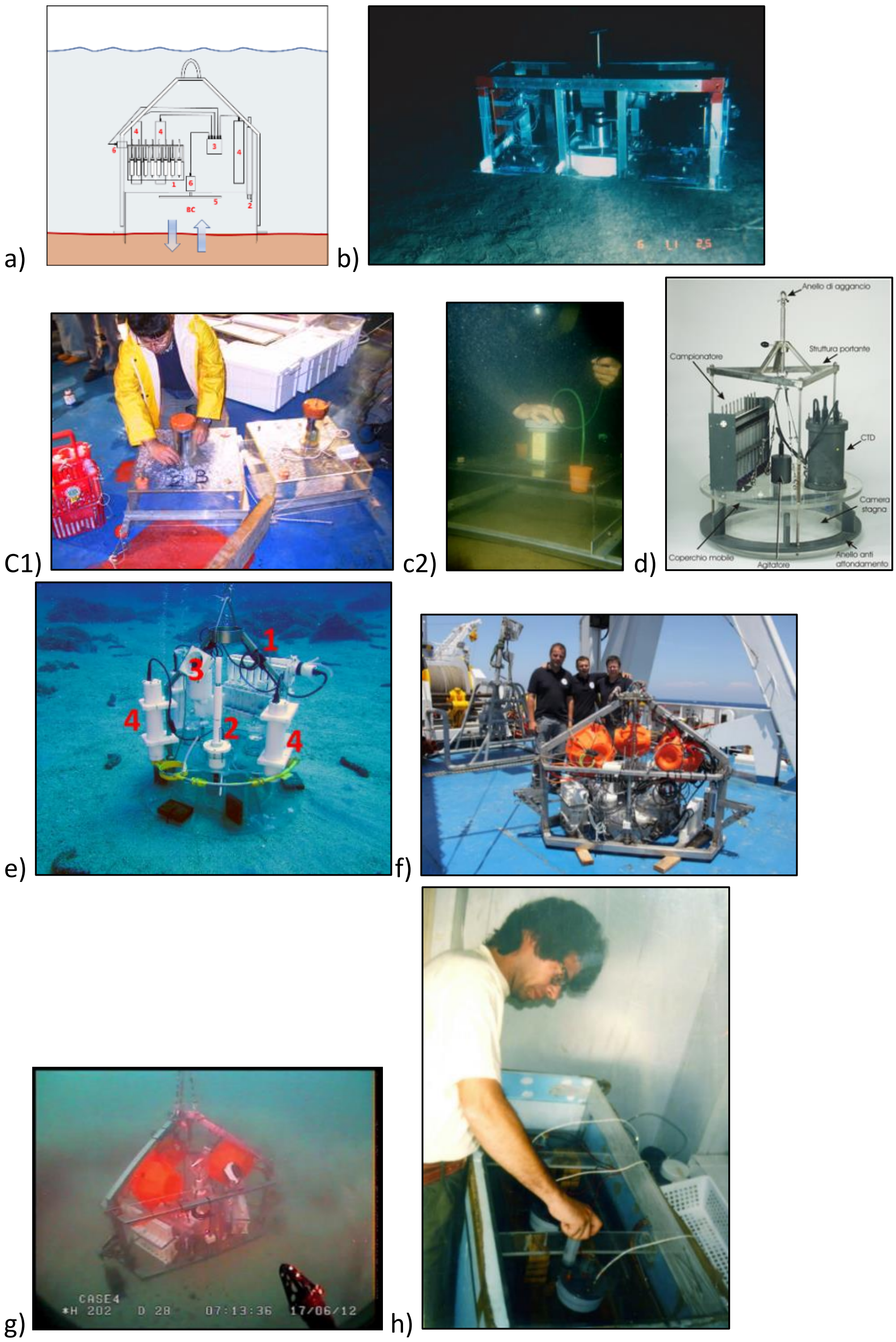

Figure S4. a) Schematic drawing of a benthic chamber (Spagnoli *et al.*, 2018, 2019). BC, Benthic Chamber: 1) Device for collecting water samples inside and outside the chamber or to inject tracers into the chamber (Vampire); 2) multiparameter probe (*Hydrolab MS5*) to measure oxygen, pH, Eh, temperature, conductivity (*i.e.* salinity) and pressure (depth) in the chamber; 3) housing of the electronics (Idec MicroSmart FC6A PLC); 4) housings of batteries; 5) rotating paddle; 6) motors. b-

g) Evolution of the benthic chamber technology at the Italian CNR: b) Benthic lander deployed on the Adriatic seafloor in 1982 (Berelson and Hammond, 1986) (credit, Gabriele Marozzi); c) first manual benthic chambers involving sampling by divers; d) first automatic benthic chamber developed at IGM-CNR of Bologna (Masini *et al.*, 2001); e) the AdaN chamber (Spagnoli *et al.*, 2018, 2019). f) the Amerigo lander on deck; g) the Amerigo deployed on the seafloor (Spagnoli *et al.*, 2018, 2019). h) incubation of cores for the measurement of dissolved fluxes at the sediment-water interface in a thermostatic box.

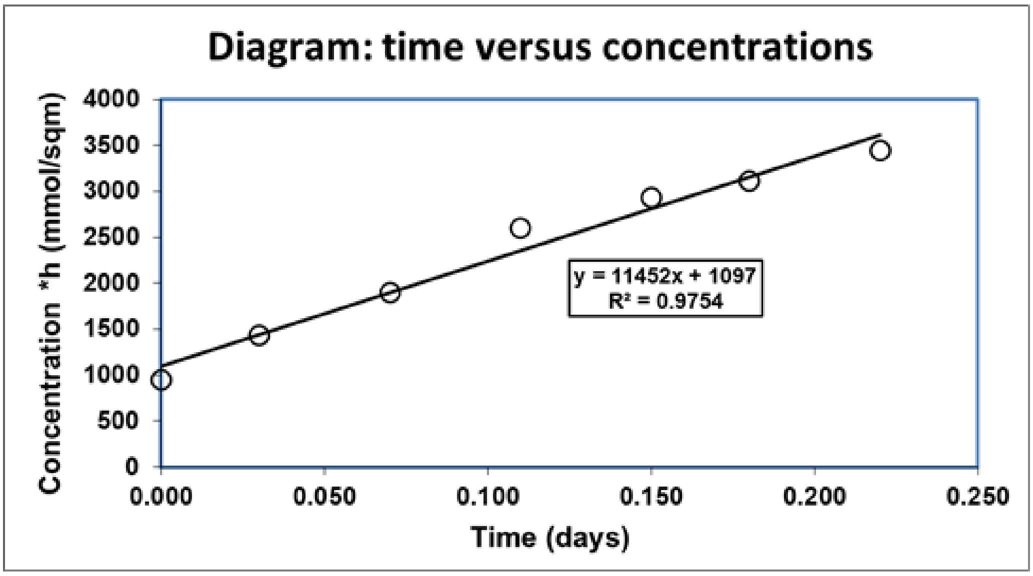

Figure S5. Concentrations of chemical compound i^{th} versus time; m is the angular coefficient of the straight line calculated by the minimum square method.

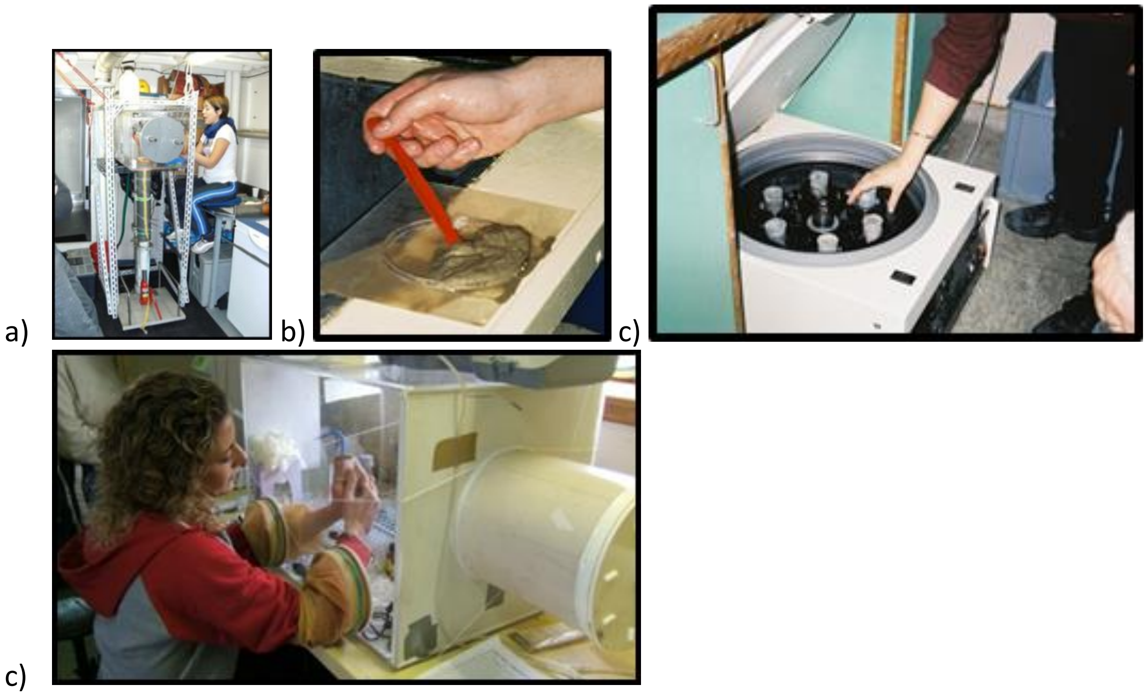

Figure S6. a) Pictures of some steps of the collection of pore waters from sediment cores by the SW104 corer. a) the sediment core mounted on the extrusion frame with its top in the inert gas glove box; b) subsampling of the sediment core slices; c) centrifugation of sediment slices d) pore water filtration, aliquot preparation poisoning and acidification in the inert gas glove box.

a) 

b) 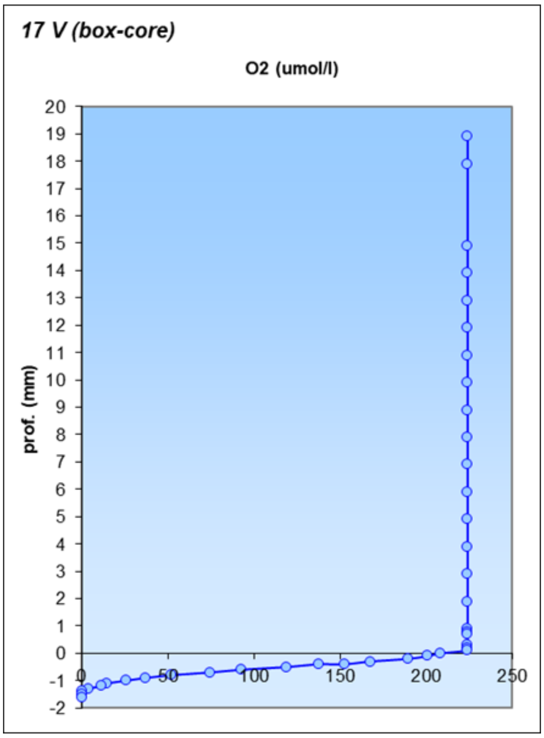

Figure S7. On-board profiling at the sediment-water interface on a core by a microelectrode (CNR, Cruise Vector 632). a) micro-profiling apparatus; b) drawing of the results (O2 concentrations).

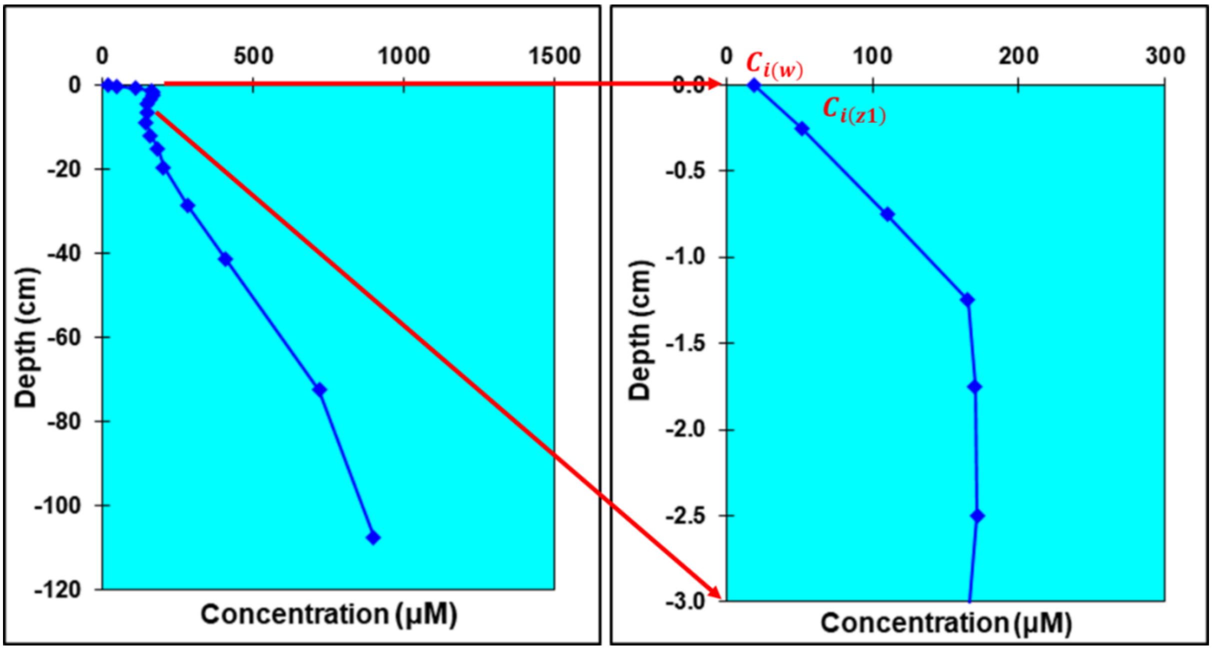

Figure S8. Pore water and bottom water concentration profile of chemical compound i^{th} obtained from pore water extraction.

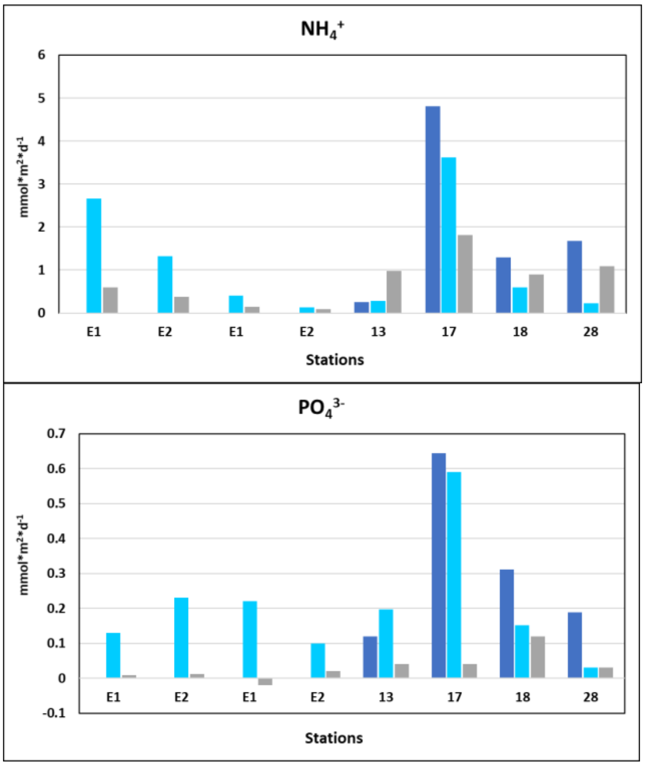

Figure S9. DFSWIs of NH_4^+ and PO_4^{3-} measured by *in situ* benthic chamber deployments (blue), by on-board core incubation (clear blue), and by pore water modeling (grey) at the same station in the same season. See Figure S3 for station locations.

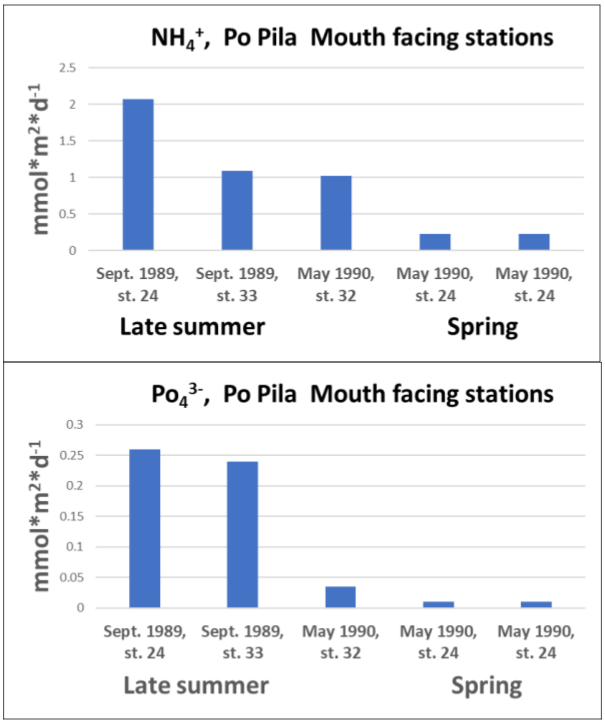

Figure S10. Variability of NH_4^+ and PO_4^{3-} DFSWIs in different seasons (summer and spring) at stations located in the same area (in this case, facing the *Po di Pila* mouth). See Figure S3 for station locations.

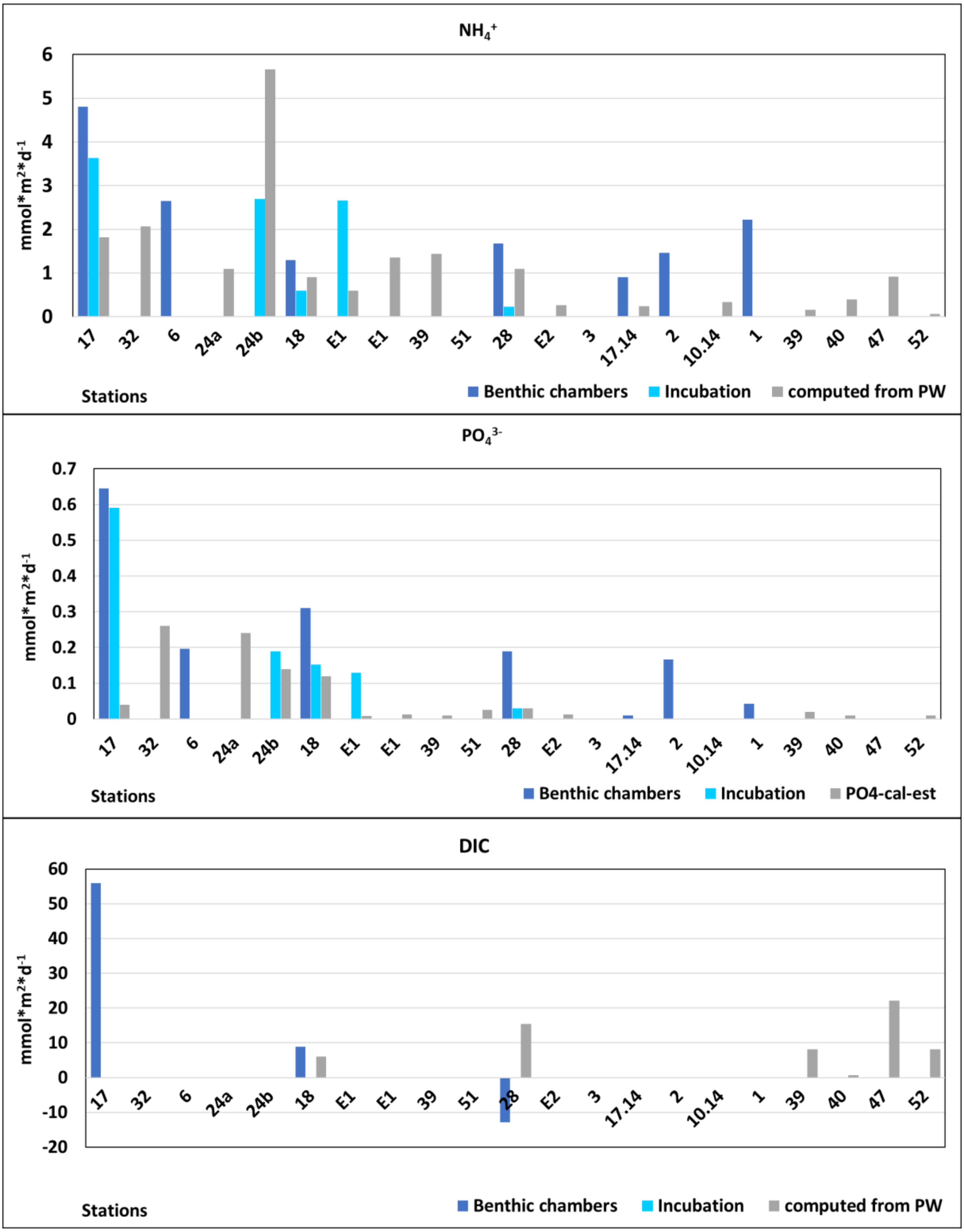

Figure S11. DFSWIs of organic matter degradation products (NH_4^+, DIC, PO_4^{3-}) at stations located along the Holocene mud wedge on the Adriatic seafloor, between the Po River Delta (left) and the MAD (right), in late summer. Blue: in situ deployments, light blue: on-board incubations, grey: pore water calculations. PW, Pore Water.

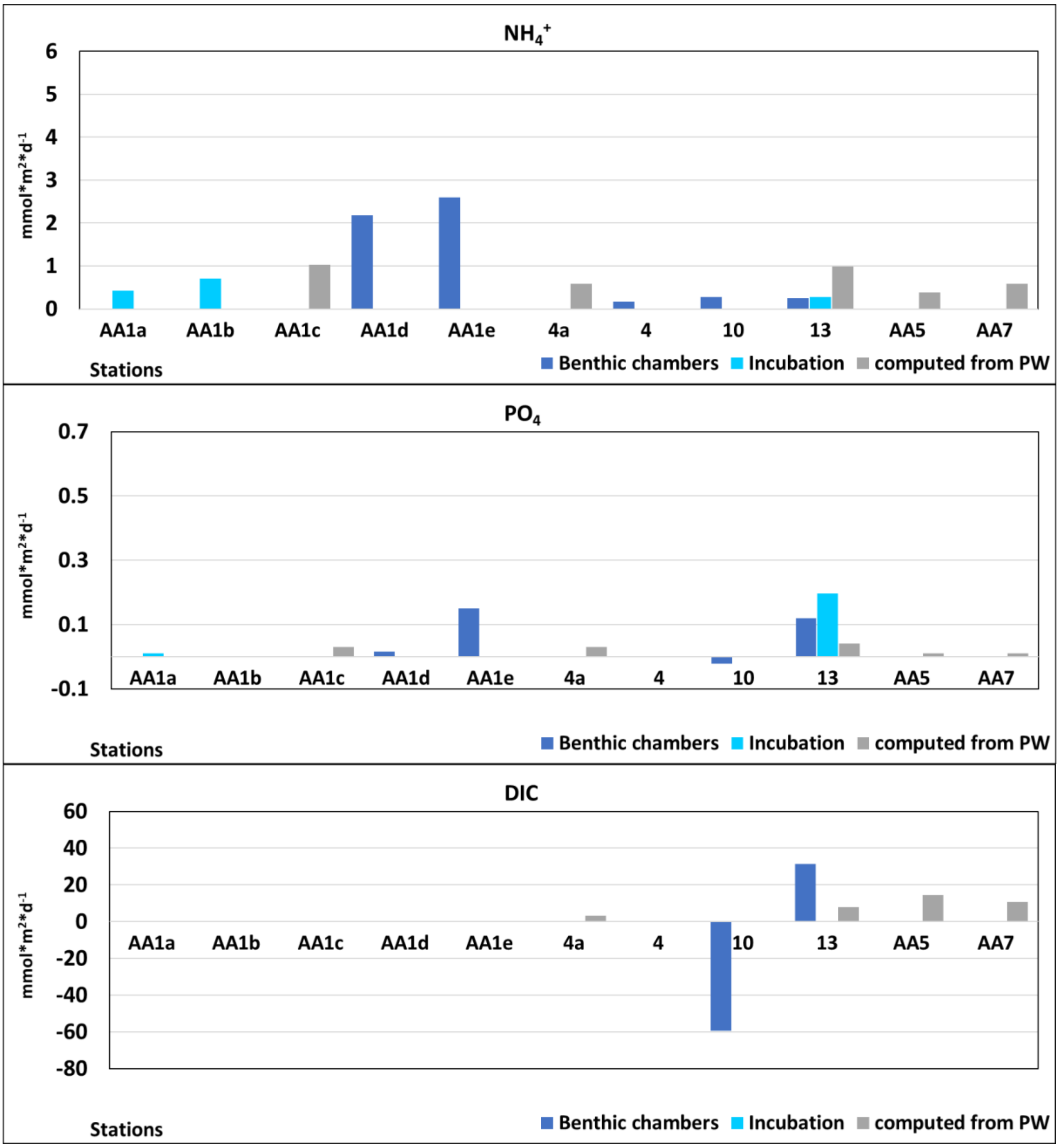

Figure S12. DFSWIs of organic matter degradation products (NH_4^+, DIC, PO_4^{3-}) on the Adriatic seafloor north of the Po Delta and offshore in the Central Adriatic. PW, Pore Water.

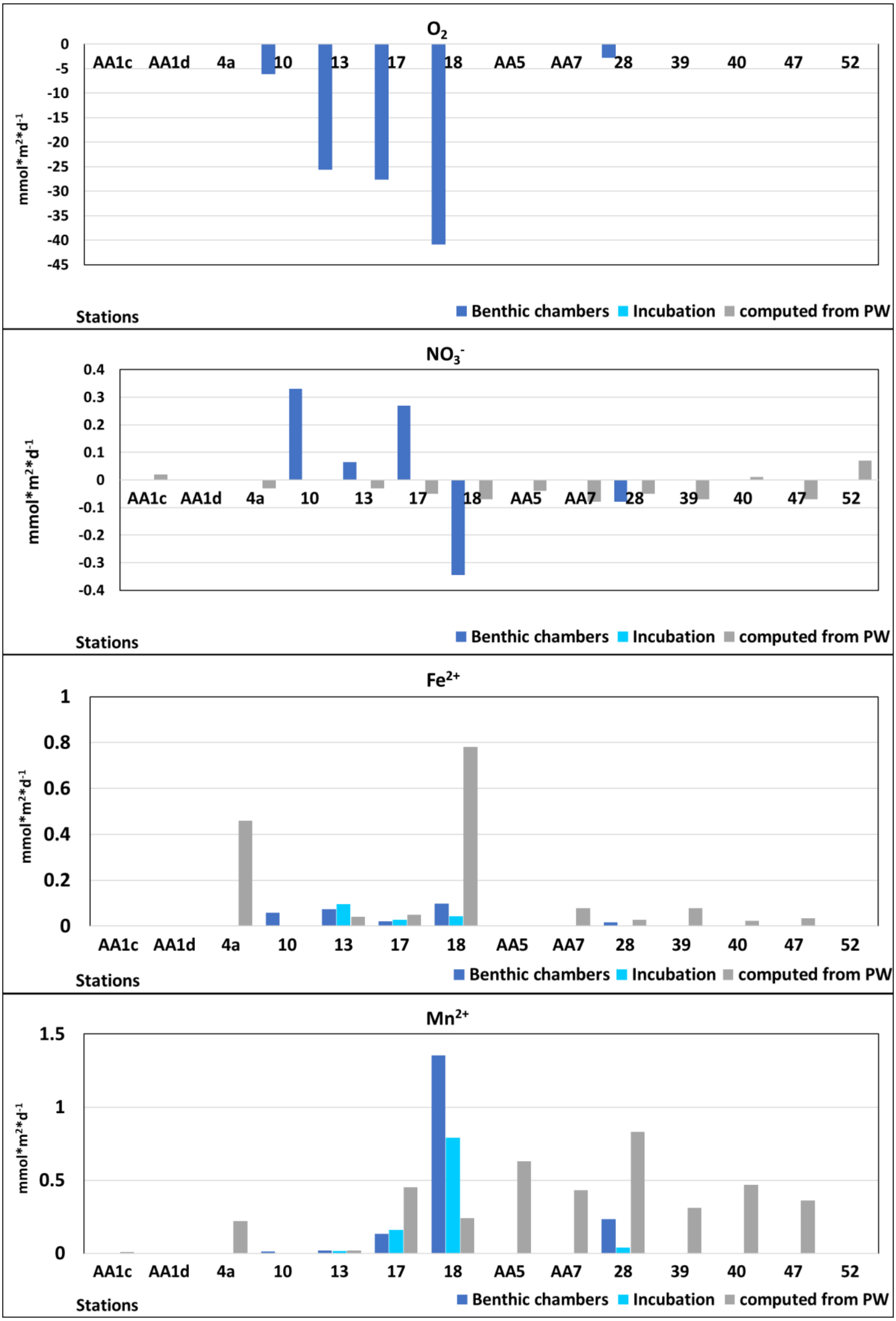

O_2
NO_3^-
Fe^{2+}
Mn^{2+}
mmol*m²*d⁻¹
Stations
AA1c AA1d 4a 10 13 17 18 AA5 AA7 28 39 40 47 52
Benthic chambers
Incubation
computed from PW

Figure S13. DFSWIs of the final electron acceptors (O_2, NO_3^-, Fe, Mn) at the station established on the Adriatic seafloor. PW, Pore Water.

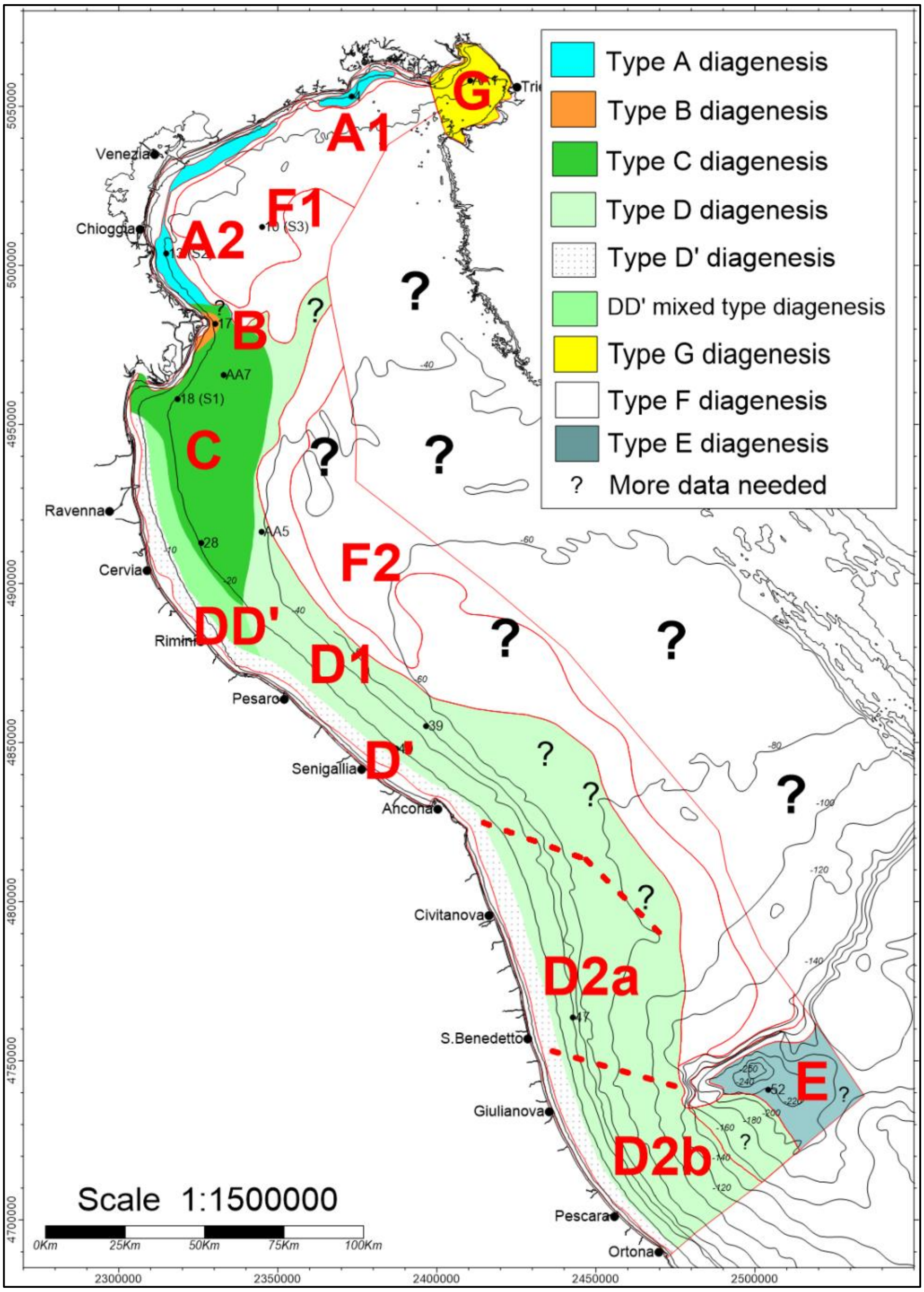

Figure S14. Areas characterized by different early diagenesis processes and flux intensities at the water-sediment interface in the Adriatic Sea. Question marks indicate areas where the available data are insufficient for classification.

Table S1. Dissolved fluxes at the sediment-water interface as measured and calculated from pore water profiles in the Northern and Central-Western Adriatic Sea.

Units: $mmol*m^{-2}*d^{-1}$.

Date	Stations		Season	Latitude	Longitude	NH_4^-			PO_4^{3-}			DIC		
				DD.dddd	DD.dddd	Benthic chambers	Core Incubation	Computed from PW	Benthic chambers	Core Incubation	Computed from PW	Benthic chambers	Core Incubation	Computed from PW
April, 1982	10.14	DD'	Spring	44.2511	12.5844			0.490			0.002			
April, 1982	17.14	DD'	Spring	44.2792	12.5983			0.165			0.002			
June, 1982	10.14	DD'	Late Spring	44.2511	12.5844			0.340			0.001			
June, 1982	17.14	DD'	Late Spring	44.2792	12.5983	0.900		0.235	0.010		0.000			
September, 1988	1	D'	Late Summer	44.2263	12.4688	2.220			0.043					
September, 1988	2	C	Late Summer	44.2567	12.5397	1.460			0.167					
September, 1988	3	C	Late Summer	44.2917	12.6398									
September, 1988	4	F2	Late Summer	44.3733	12.8725	0.170			-0.001					
September, 1988	6	C	Late Summer	44.7458	12.4000	2.650			0.197					
September, 1988	7	C	Late Summer	44.7458	12.5000	0.660			0.046					
September, 1989	7	D1/C	Late Summer	44.2001	12.7523			0.340			0.017			
September, 1989	16	C	Late Summer	44.4791	12.5104			0.360			0.009			
September, 1989	24	C	Late Summer	44.7410	12.4525			1.090			0.240			
September, 1989	32	B	Late Summer	44.9660	12.5801			2.070			0.260			
May, 1990	7	D1/C	Spring	44.2001	12.7523			0.180			0.022			
May, 1990	32	B	Spring	44.9660	12.5801			1.020			0.035			
May, 1990	24	C	Spring	44.7410	12.4525			0.230			0.010			
May, 1990	16	C	Spring	44.4791	12.5104			0.140			0.007			
September, 1992	24	C	Late Summer	44.7375	12.4619		2.690	5.660		0.190	0.140			
October, 1992	AA1a	G	Fall	45.6667	13.5942		0.420			0.010				
December, 1992	AA1f	G	Winter	45.6667	13.5942		-0.400			-0.025				
March, 1992	1/S1	C	Spring	44.7373	12.4583	20								
March, 1992	2/S2	C	Spring	44.7530	12.5000	58/30								
March, 1992	3/S3	C	Spring	44.3347	12.6658	0								
March, 1992	5/S5	D1	Spring	43.9417	13.2233	22/11-								
March, 1992	6/S6	D1	Spring	43.7033	13.6417	11/5-								
March, 1992	10/P1	E	Spring	42.8500	14.7500									
August, 1993	11 /S11	B	Summer	42.8500	12.6500	53	29							
August, 1993	2/S2	C	Summer	44.0967	12.5000	23	30							
August, 1993	3/S3	C	Summer	44.3333	12.6658	86	101							
August, 1993	4/S4	F2	Summer	44.3733	12.8725	<20	<10							
August, 1993	5/S5	D1	Summer	43.9417	13.2233	<10	<10							
August, 1993	6/S6	D1	Summer	43.7033	13.6417	<20	<10							
August, 1993	8	D2	Summer	42.7348	14.1650		<10							
August, 1993	10/P1	E	Summer	42.8500	14.7500		<10	0.07			0.002			
February, 1993	26	DD'	Late Winter	44.3860	12.4510			0.498			0.006			
February, 1993	39	DD'	Late Winter	44.3801	12.4542			0.927			0.002			
February, 1993	51	DD'	Late Winter	44.3575	12.4722			0.926			0.010			
April, 1993	AA1g	G	Spring	45.6667	13.5942		0.150			-0.010				
July, 1993	AA1b	G	Summer	45.6667	13.5942		0.700			0.001				
September, 1993	26	DD'	Late Summer	44.3854	12.4512			1.806			0.018			
September, 1993	39	DD'	Late Summer	44.3783	12.4553			1.440			0.010			
September, 1993	51	DD'	Late Summer	44.3581	12.4717						0.025			
February, 1994	E1	C	Late Winter	44.5442	12.4506			0.400			0.012			
February, 1994	E2	C	Late Winter	44.3069	12.5781			0.620			0.001			
February, 1994	E3	D1/D'	Late Winter	43.7150	13.4456			0.620			0.003			
February, 1994	E4	D2?	Late Winter	42.2767	14.9044			0.440			0.002			
Juy, 1994	E1	C	Summer	44.5442	12.4506		2.660	0.590		0.130	0.008			
July, 1994	E2	C	Summer	44.3069	12.5781		1.320	0.380		0.230	0.013			
July, 1994	E3	D1/D'	Summer	43.7150	13.4456		18.400	0.100		0.190	0.010			
July, 1994	E4	D2?	Summer	42.2767	14.9044		3.200	0.040		-0.040	0.003			
September, 1994	E1	C	Late Summer	44.5442	12.4506			1.360			0.012			
September, 1994	E2	C	Late Summer	44.3069	12.5781			0.259			0.013			
September, 1994	E3	D1/D'	Late Summer	43.7150	13.4456			0.551			0.003			
February, 1995	E1	C	Late Winter	44.5442	12.4506			0.185			0.003			
February, 1995	E2	C	Late Winter	44.3069	12.5781			0.246			0.009			
February, 1995	E3	D1/D'	Late Winter	43.7150	13.4456			0.261			-0.001			
April, 1995	E1	C	Spring	44.5442	12.4506		0.400	0.150		0.220	-0.020			
April, 1995	E2	C	Spring	44.3069	12.5781		0.130	0.090		0.100	0.020			
April, 1995	E3	D1/D'	Spring	43.7150	13.4456		0.170			-0.090				
April, 1995	E4	D2	Spring	42.2767	14.9044		0.080			0.880				
October 1995	AA1c	G	Fall	45.6667	13.5942			1.020			0.030			
October, 1995	AA1d	G	Fall	45.6667	13.5942	2.178			0.016					
October, 1995	4a	A1	Fall	45.6148	13.1175			0.590			0.030			3.091
October, 1995	10a	F1	Fall	45.2396	12.7714	0.273			-0.022			-59.370		
October, 1995	13	A2	Fall	45.1565	12.3910	0.247	0.276	0.980	0.119	0.197	0.040	31.280		7.935
October, 1995	17	B	Fall	44.9619	12.5953	4.806	3.626	1.820	0.645	0.591	0.040	55.955		
October, 1995	18	C	Fall	44.7460	12.4545	1.296	0.591	0.900	0.311	0.153	0.120	8.905		6.049
October, 1995	AA5	D1	Fall	44.3776	12.8024			0.380			0.010			14.474
October, 1995	AA7	C	Fall	44.8180	12.6348			0.590			0.010			10.765
October, 1995	28	C	Fall	44.3415	12.5657	1.676	0.225	1.090	0.189	0.030	0.030	-12.855		15.413
October, 1995	39a	D1	Fall	43.8387	13.4653			0.160			0.020			8.502
October, 1995	40	D1	Fall	43.7733	13.3502			0.390			0.010			0.695
October, 1995	47	D2	Fall	43.0206	14.0518			0.920			0.000			22.062
October, 1995	52	E	Fall	42.8198	14.8065			0.060			0.010			8.105
December, 1995	AA1h	G	Winter	45.6667	13.5942	0.486			0.005					
April, 1996	AA1g	G	Spring	45.6667	13.5942	0.015			0.002					
July, 1996	AA1e	G	Summer	45.6667	13.5942	2.600			0.150					
march, 1996	F	G	winter	45.5382	13.5500		0.71			0.04			5.02	
September 1996	F	G	summer	46.5382	14.5500		1.4			0.03			7.565	
1995-	E11	C		44.9675	12.5833									
March, 1998	10/P1	E	Spring	42.8500	14.7500			0.243			0.005	4		